

*Nikola Vladimir
Ivo Senjanović
Neven Alujević
Dae-Seung Cho
Jose Luis Mantari Laureano*

<https://doi.org/10.21278/TOF.43107>
ISSN 1333-1124
eISSN 1849-1391

STRUCTURAL INTEGRITY OF AN AGED OIL TANKER CONVERTED INTO THE PORT OIL STORAGE

Summary

A procedure for strength assessment of a ship structure partially grounded in mud is developed. The paper deals with a practical engineering problem of evaluating the structural integrity of a single bottom tanker which, after its regular service, was grounded in mud and continued to be used as oil storage in order to increase the storage capacity of the port. A mathematical model of the ship static equilibrium is formulated, consistently taking into account the ship, the cargo and ballast weights, the supporting mud reaction, and the surrounding water buoyancy. For simplicity, the global strength assessment is done using the beam model, where the calculation of ship sectional properties is performed by the specialized in-house software. Subsequently, the developed model is used as a basis for a detailed 3D FEM analysis. The thickness measurements of the complete ship structure were performed in order to directly account for the corrosion effect.

Key words: *single hull oil tanker, oil storage, corrosion, structural analysis, FEM.*

1. Introduction

Demolition of aged ships is an important strategy for balancing the fleet capacity in the shipping sector [1]. As discussed by Yin and Fan [1], it is influenced by the ship obsolescence, technical developments, and environmental regulations on ship demolition, as well as by the state of the shipping market in general and by operating costs. A similar conclusion can also be drawn from the studies done by Stott [2] and Schøyen et al. [3]. Instead of submitting aged tankers to the usual recycling process, which is nowadays the subject of different policies [4], their hulls can sometimes be used to increase storage capacities in ports if this is economically justified [5]. However, one should take care about the ship hull integrity because of human safety during operation and potential environmental issues [6]. Generally speaking, a primary concern in the maritime sector is to enhance ship safety and to reduce marine pollution related to ship incidents and accidents [7]. In this process, the hull inspection is a very important task. Namely, it is well-known that corrosion affects both the local and the global ship strength so that a number of models have been

developed in order to improve the structural analysis, inspection, and maintenance procedures as reported in [8,9,10,11]. Moreover, corrosion is one of the time-dependent detrimental phenomena which can lead to catastrophic failures [11,12,13].

This paper is focused on the practical problem of strength assessment of a grounded, aged, single-hull oil tanker, which is being used as the port oil storage. Namely, after its regular service, the ship was converted in such a way that its cargo area module is used as a stationary object with the aim of increasing the port storage capacities. The outline of a theoretical model with some selected 3D FEM results was presented in the conference paper [14]. The developed theoretical model is based on static equilibrium and geometric relations; in the model, the mud mass density is adjusted in order to properly take into account the sea bottom stiffness, i.e. the bottom reaction force. This is done because it was confirmed by observations that the exact ship position is independent of the loading condition variation. Therefore, it is reasonable to conclude that the mud reaction continuously changes depending on the cargo filling levels.

Although the developed theoretical procedure originates from a practical problem, it can be also useful for applications to similar problems such as, for instance, the salvage of ships in shallow waters. Although every grounding or stranding event is unique [15,16], in many cases, it is useful to know the exact value of contact force between the ship and the sea bottom [17], which can be precisely determined by the presented procedure.

2. Theoretical model

A single hull tanker vertically immersed in mud and surrounded by the sea water is presented in Fig. 1.



Fig. 1 Schematic diagram of the ship position [14]

The weight of the grounded ship is equilibrated partly by the buoyancy of water and partly by the sea bottom reaction. Hence, the total reaction $R=F-B$, as a difference between the ship weight, F , and the buoyancy, B , is known, but its distribution along the ship is not. In the proposed procedure it is assumed that the ship hull freely floats both in water and in mud, Fig. 2, [14].

The ship weight, F , has to be equilibrated by the buoyancy of the water and the mud, respectively:

$$F = \rho_w g \int_0^L A_w(x) dx + \rho_m g \int_0^L A_m(x) dx, \quad (1)$$

which gives:

$$F = \rho_w g V_w + \rho_m g V_m, \quad (2)$$

where ρ_w and ρ_m denote the density of the water and the mud, respectively. In addition, V_w and V_m represent the volume of the ship immersed in the water and the mud, respectively, while A_w and A_m denote the cross-section area immersed in the water and the mud, respectively. The gravity constant is denoted by g .

From Eq. (2), one can calculate the mud density necessary to maintain the static equilibrium:

$$\rho_m = \frac{F - \rho_w g V_w}{g V_m} \quad (3)$$

In the case of unit immersion of a ship, additional buoyancy represents the sea bottom (mud) stiffness, and yields:

$$k = \rho_m g B_m \quad (4)$$

where B_m is the cross-section breadth at the borderline between the mud and the water, Fig. 2.

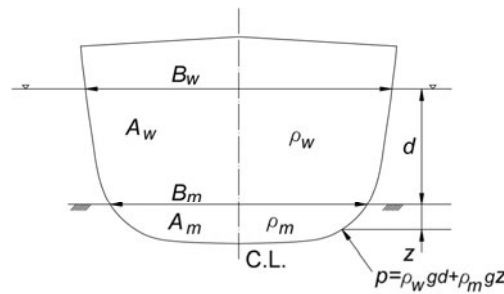


Fig. 2 Cross-section of a ship immersed in the water and the mud [14]

2.1 Determination of the mud pressure

The distribution of the mud reaction along the ship hull is shown in Fig. 3a. It can be calculated by knowing the total weight of the ship and the cargo, F , and the longitudinal position of the centre of gravity (CG), x_{CG} , which are regularly available from the loading manual.

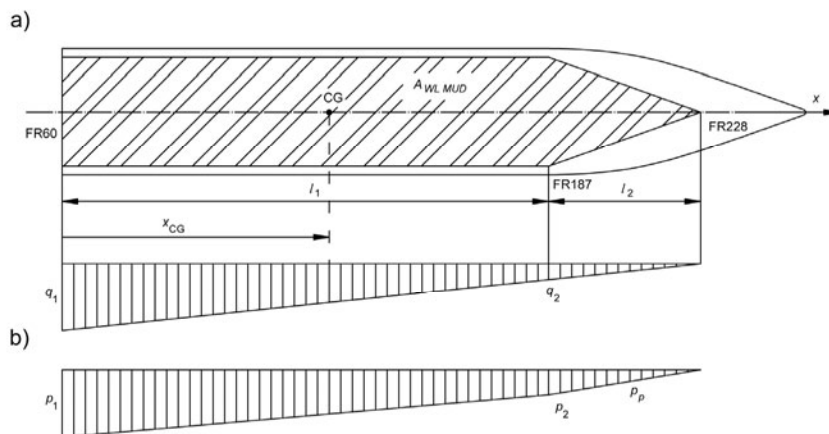


Fig. 3 Mud reaction (a) and the mud pressure distribution (b) along the ship

According to Fig. 3a, the following expressions are obtained from the force and moment equilibrium:

$$q_1 + q_2 \left(1 + \frac{l_2}{l_1} \right) = \frac{2F}{l_1} \quad (5)$$

$$q_1 + q_2 + 2q_2 \frac{l_2}{l_1} \left(l_1 + \frac{1}{3} l_2 \right) = \frac{4}{l_1^2} F x_{CG} \quad (6)$$

which leads to:

$$q_1 + q_2 \left[1 + 2 \frac{l_2}{l_1} \left(1 + \frac{1}{3} \frac{l_2}{l_1} \right) \right] = \frac{4}{l_1^2} F x_{CG}. \quad (7)$$

After substituting (5) into (7), one can write:

$$q_2 \frac{l_2}{l_1} \left(1 + \frac{2}{3} \frac{l_2}{l_1} \right) = \frac{2F}{l_1} \left(2 \frac{x_{CG}}{l_1} - 1 \right). \quad (8)$$

Based on the above derivation, q_2 and q_1 can be expressed as:

$$q_2 = \frac{\frac{2F}{l_1} \left(2 \frac{x_{CG}}{l_1} - 1 \right)}{\frac{l_2}{l_1} \left(1 + \frac{2}{3} \frac{l_2}{l_1} \right)}, \quad q_1 = \frac{2F}{l_1} - q_2 \left(1 + \frac{l_2}{l_1} \right). \quad (9)$$

For the pressure calculation, the width of the mud waterline, B_{WLMUD} , is relevant, Fig. 3a. According to Fig. 3b, one can write for the first, the second, and generally for the i -th tank area:

$$p_1 = \frac{q_1}{B_{WLMUD}}, \quad p_2 = \frac{q_2}{B_{WLMUD}}, \quad p_i = \frac{q_i}{B_i}. \quad (10)$$

2.2 An outline of the 1D FEM procedure

For the 1D FEM analysis, an in-house code has been developed based on the Timoshenko beam theory [18]; the analysis is performed by the finite element method [19,20]. The two-node finite element equation reads, [19,20]:

$$\{F_e\}_q - \{F_e\}_b = [K]\{\delta\} + [K]_r\{\delta\}, \quad (11)$$

where $\{F\}$ denotes the nodal force vector, and $\{\delta\}$ represents the vector of nodal displacements. The ordinary stiffness matrix for bending and shear from [19] is used, while the restoring matrix reads:

$$[K]_r = \frac{kl}{420(1+12\beta)^2} \begin{bmatrix} 156 + 3528\beta + 20160\beta^2 & (22 + 462\beta + 2520\beta^2)l & 54 + 1512\beta + 10080\beta^2 & -(13 + 378\beta + 2520\beta^2)l \\ & (4 + 84\beta + 504\beta^2)l^2 & (13 + 378\beta + 2520\beta^2)l & -(3 + 84\beta + 504\beta^2)l^2 \\ & & 156 + 3528\beta + 20160\beta^2 & -(22 + 462\beta + 2520\beta^2)l \\ Sym. & & & (4 + 84\beta + 504\beta^2)l^2 \end{bmatrix}, \quad (12)$$

where k represents the mud stiffness and $\beta = EI / GA_s l^2$.

The buoyancy vector yields:

$$\{F_e\}_b = \frac{b_1 l}{60(1+12\beta)} \begin{bmatrix} 3(7-120\beta) \\ 3(1+10\beta)l \\ 3(3-40\beta) \\ -2(1+15\beta)l \end{bmatrix} + \frac{b_2 l}{60(1+12\beta)} \begin{bmatrix} 3(3+40\beta) \\ 2(1+15\beta)l \\ 3(7+120\beta) \\ -3(1+10\beta)l \end{bmatrix}, \quad (13)$$

where b_1 and b_2 represent the buoyancy values at the beginning and the end of FE, respectively. Similarly, for the weight vector with uniform weight distribution, one can write:

$$\{F_e\}_q = \frac{ql}{60(1+12\beta)} \begin{Bmatrix} 30(1-8\beta) \\ 5(1+12\beta)l \\ 30(1+8\beta) \\ -5(1+12\beta)l \end{Bmatrix}. \quad (14)$$

After acquiring the global stiffness, restoring matrices, and loading vectors, the hull deflection is obtained:

$$\{\tilde{\delta}\} = \left([\tilde{K}] + [\tilde{K}]_r \right)^{-1} \left(\{\tilde{F}_e\}_q - \{\tilde{F}_e\}_b \right). \quad (15)$$

Finally, after determining the displacement vector $\{\tilde{\delta}\}$, the nodal shear forces and bending moments can be obtained by returning to the finite element equation, Eq. (11).

3. Ship data, description of calculation setup and FEM models

3.1 Ship data

The considered ship was built in 1956, with the tank layout shown in Fig. 4 and the following main particulars:

Length between perpendiculars:	$L_{PP} = 149.07$ m,
Breadth:	$B = 25.72$ m,
Depth to the main deck:	$H = 14.1$ m.

The central cargo tanks 4C-9C are intended to be used as the oil storage. The side tanks 1L, 1D, 4L, and 4D are to be empty, whereas the tanks 2L, 2D, 3L, 3D, 5L, 5D, 6L, and 6D contain permanent ballast, which together with the lightship mass, ensure a permanent contact between the ship structure and the bottom, [14].

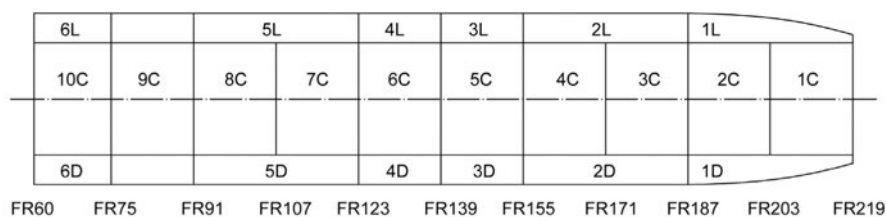


Fig. 4 Ship arrangement with the disposition of tanks
 (C – central tanks, L – port side tanks, D – starboard tanks)

Thickness measurement of the entire structure of the ship has been performed in order to accurately take into account the corrosion effect, i.e. to reliably simulate a realistic ship condition. For illustration, the arrangement of measurement points for the side tank plating is shown in Fig. 5. The ship is made of steel; for the purpose of calculation, the values of Young's modulus, material density, and Poisson's ratio are set at 2.1×10^{11} N/m², 7850 kg/m³, and 0.3, respectively.

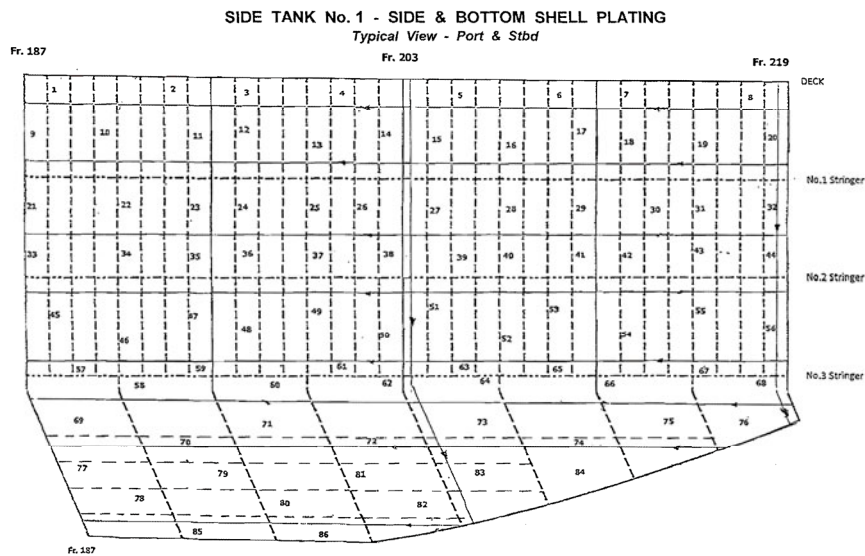


Fig. 5 Arrangement of measurement points for a side tank

3.2 Calculation setup

For both the global and the local strength assessment, two sets of different representative loading conditions are defined. For the global strength assessment, the ship is considered as a beam, and it is reasonable to assume that critical loading conditions are those representing a beam subjected to concentrated forces. In this sense, the loading conditions LC1 and LC2, Fig. 6a and 6b, are defined. Since the aims of the global and the local strength assessments are different, separate loading conditions should be considered in the 3D FEM analysis. In the local strength assessment, it is reasonable to assume that critical loading conditions are those causing maximum stresses in the transverse bulkheads, as shown in Fig. 6c and 6d.

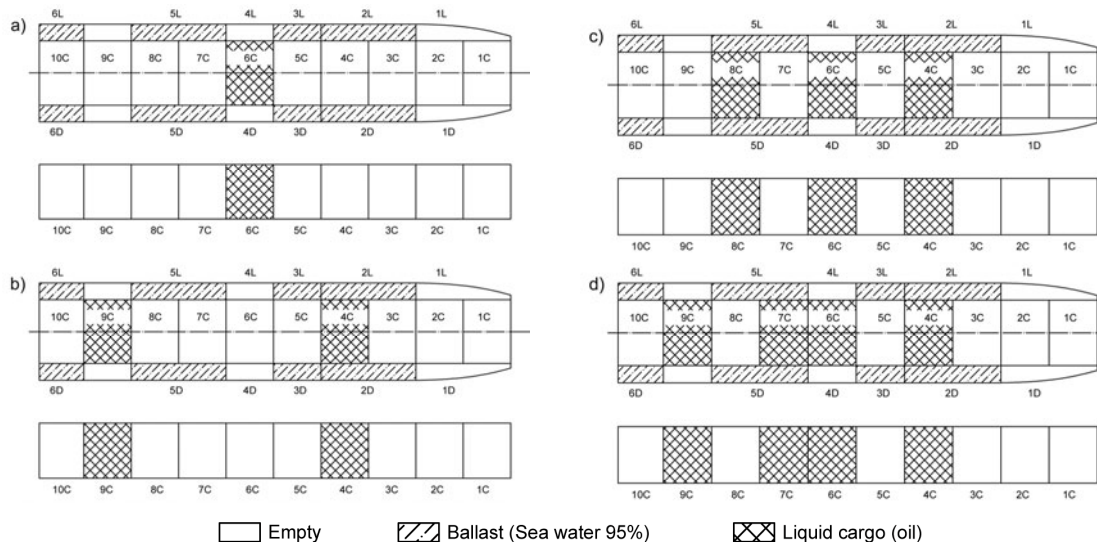


Fig. 6 Schematic diagram of load cases

3.3 1D FEM model

Stiffness parameters of the ship hull cross-section are determined using the strip element method [21]; the software used here is the in-house software STIFF [22], Fig. 7.

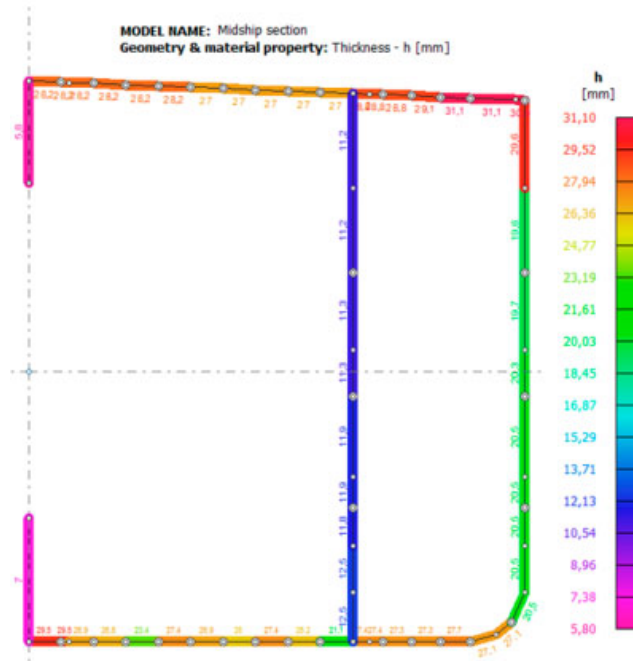


Fig. 7 Averaged thickness of plating at the midship section – STIFF software

The developed in-house code is used to determine global deflections of the ship structure supported by the mud and surrounded by the sea water. The beam model consists of 20 finite elements, where each tank is modelled with 2 finite elements. Longitudinal weight distributions for LC1 and LC2 are given in Fig. 8 and 9, respectively, where FE nodes along the ship are also marked.

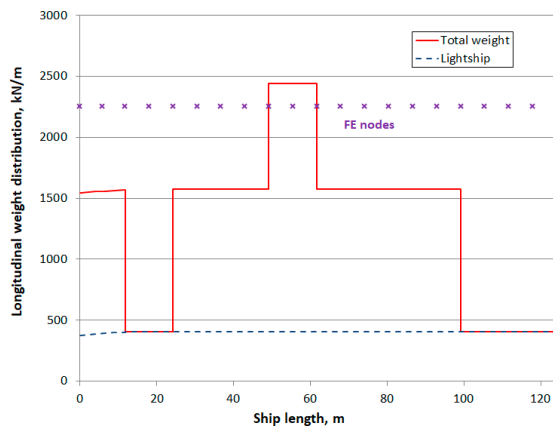


Fig. 8 Longitudinal weight distribution for LC1

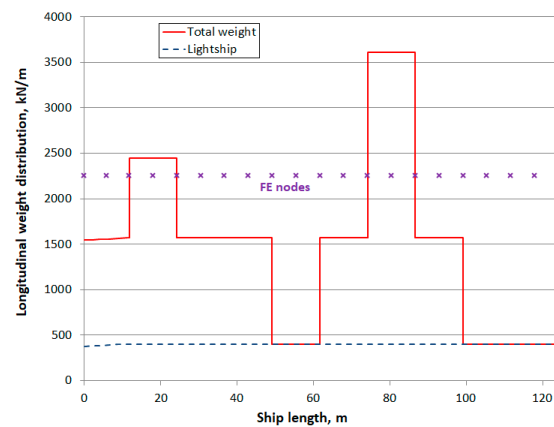


Fig. 9 Longitudinal weight distribution for LC2

3.4 3D FEM model

A fine mesh 3D FEM model is generated in order to perform a detailed strength assessment. The axonometric view on the FEM model is shown in Fig. 10. The complete FEM model was updated with ultrasonic gauging inspection data, as shown in the case of a typical cargo tank structure together with the side (ballast) tank structure, Fig. 11a, and the transverse bulkhead, Fig. 11b. Besides ordinary frames, the analysed ship structure is characterized by both semi-web frames, Fig. 12.

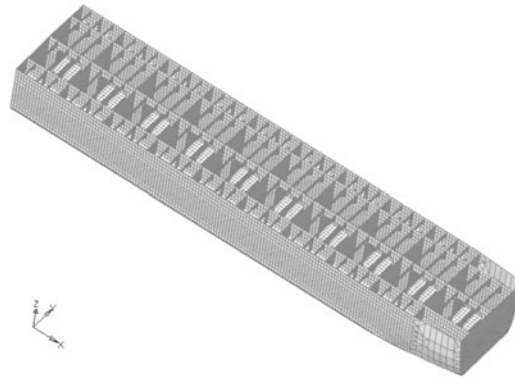


Fig. 10 3D FEM model used in the structural analysis (view without the main deck structure)

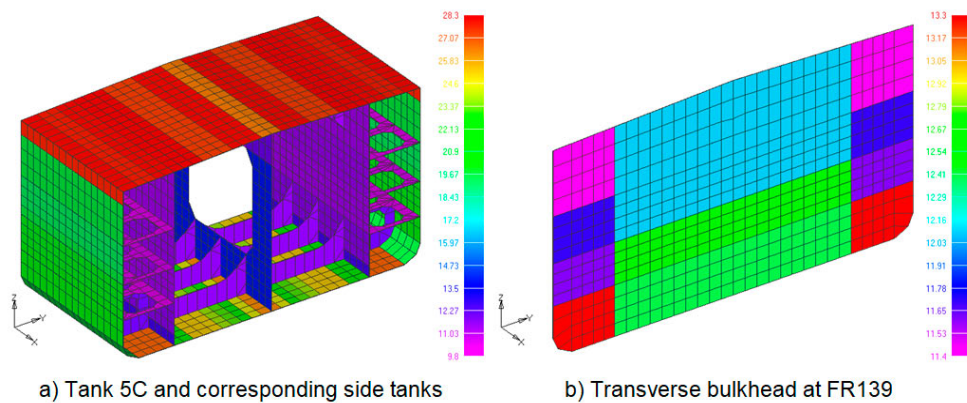


Fig. 11 Typical cargo and ballast tank structure and transverse bulkhead with indicated plate thickness (mm)

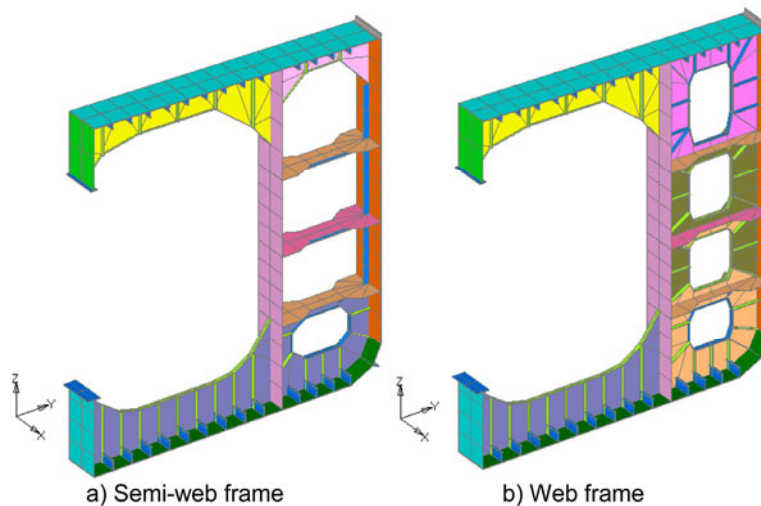


Fig. 12 Typical web frames

4. Results

The FEM results obtained by the 1D FEM model are summarized in Fig. 13, where deflections along the ship are shown. For both LC1 and LC2, static deformations are almost negligible, confirming that the longitudinal strength is not an issue for a ship continuously supported by the mud. Some significant global deformations and consequently higher stresses can be expected only if the whole ship is moved from the existing equilibrium position, which cannot be achieved only by changing the amount of cargo.

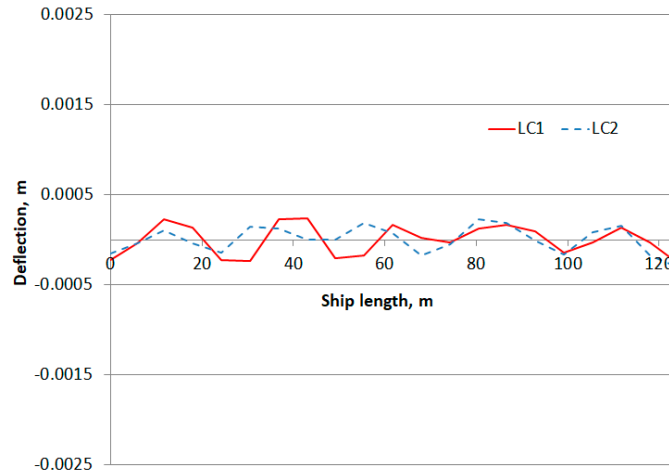


Fig. 13 Ship vertical deflections for LC1 and LC2

The 3D FEM static analysis is performed by the NASTRAN software [23] and the von Mises stresses are obtained for LC3 and LC4 in all structural elements, Table 1. The obtained stresses are compared with the maximum allowable stress which reads 230 N/mm^2 [24]. Next, an overview of the results is given, where stress distributions are shown for characteristic structural members within the cargo area. Stress units in all figures are N/m^2 . Besides the von Mises stresses in the transverse bulkheads, Fig. 14a, shear stresses are also checked, Fig. 14b. A typical von Mises stress distribution in a cargo tank area is shown in Fig. 15. Fig. 16 shows the stress distribution in a typical ballast tank structure, while Fig. 17 shows characteristic structural elements with the highest stress levels for LC4 (transverse bulkhead at FR91). Finally, Figure 18 shows the von Mises stresses in the starboard outer shell of a ship.

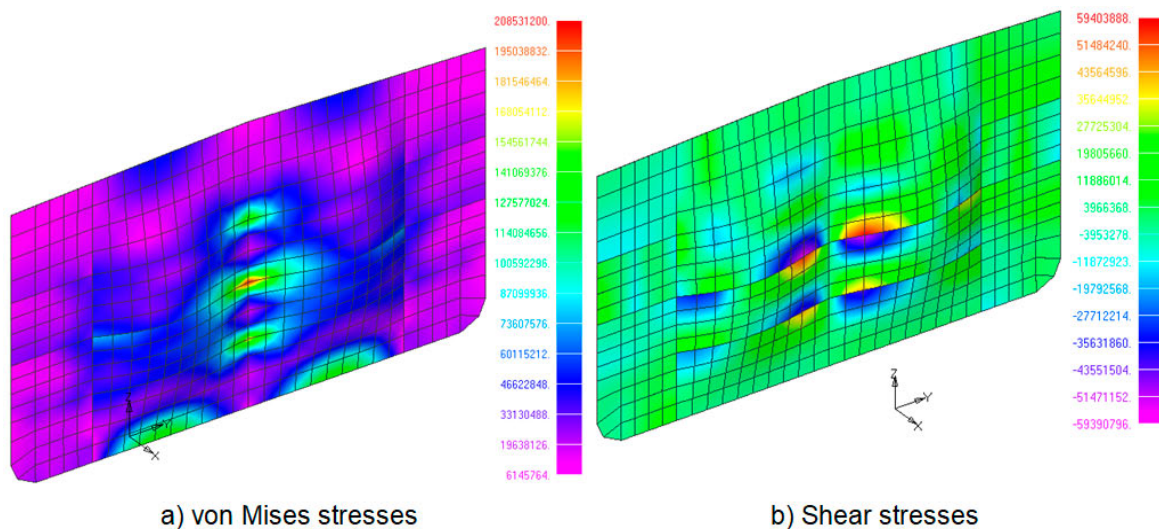


Fig. 14 Stress levels in the transverse bulkhead at FR139, LC3; a) von Mises stresses, b) shear stresses

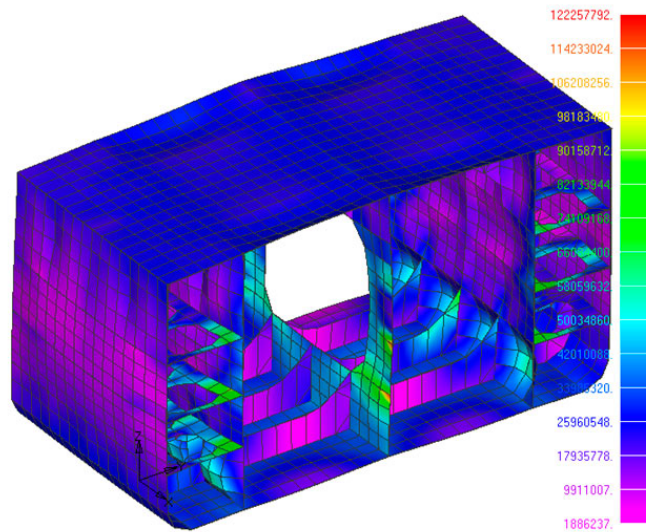


Fig. 15 Von Mises stresses in the tank 6C, LC3

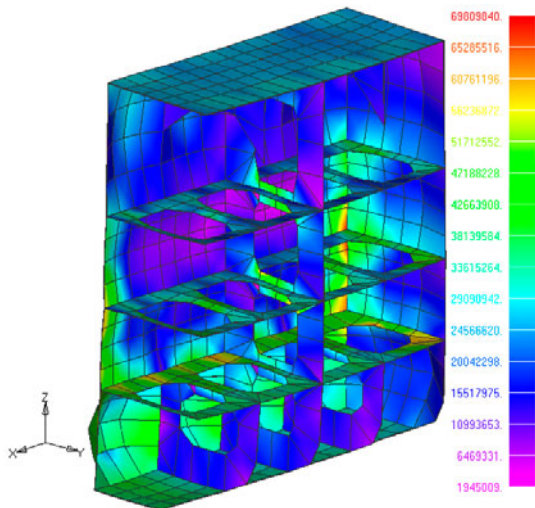


Fig. 16 Von Mises stresses in the stringers and internal walls of the tank 3L, LC3

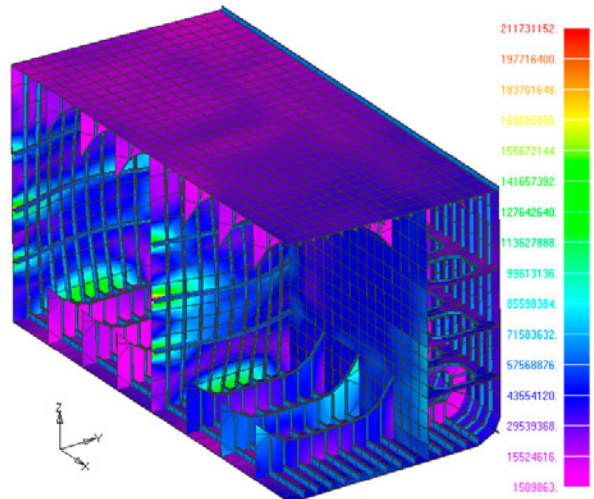


Fig. 17 Tanks 8C and 9C with transverse bulkheads at FR75 and FR91, one half of the model, LC4

Table 1 Von Mises stresses in representative structural elements obtained by the 3D FEM analysis

Name	Tank	Position along the ship	Maximum von Mises stress (N/mm ²)	
			LC3	LC4
Transverse bulkhead	10C	FR60	65.2	82.4
Transverse bulkhead	9C, 10C	FR75	35.6	189.0
Transverse bulkhead	8C, 9C	FR91	190.7	208.9
Transverse bulkhead	7C, 8C	FR107	196.7	174.9
Transverse bulkhead	6C, 7C	FR123	189.9	49.0
Transverse bulkhead	5C, 6C	FR139	208.3	208.0
Transverse bulkhead	4C, 5C	FR155	200.1	199.9
Transverse bulkhead	3C, 4C	FR171	206.3	202.6
Bottom plating	10C	FR60-FR75	123.9	184.8
Bottom plating	9C	FR75-FR91	41.1	38.0

Name	Tank	Position along the ship	Maximum von Mises stress (N/mm ²)	
			LC3	LC4
Bottom plating	8C	FR91-FR107	36.2	57.4
Bottom plating	7C	FR107-FR123	52.9	50.1
Bottom plating	6C	FR123-FR139	41.0	59.3
Bottom plating	5C	FR139-FR155	64.1	76.3
Bottom plating	4C	FR155-FR171	45.5	57.9
Bottom plating	3C	FR171-FR187	53.8	62.0
Tank internal structure	10C	FR60-FR75	97.5	138.4
Tank internal structure	9C	FR75-FR91	158.2	121.2
Tank internal structure	8C	FR91-FR107	124.7	169.3
Tank internal structure	7C	FR107-FR123	139.3	133.6
Tank internal structure	6C	FR123-FR139	132.6	142.4
Tank internal structure	5C	FR139-FR155	141.0	134.9
Tank internal structure	4C	FR155-FR171	155.4	163.1
Tank internal structure	3C	FR171-FR187	152.4	171.7
Longitudinal bulkhead, port side	10C	FR60-FR75	42.0	64.4
Longitudinal bulkhead, port side	9C	FR75-FR91	82.1	59.4
Longitudinal bulkhead, port side	8C	FR91-FR107	61.2	82.2
Longitudinal bulkhead, port side	7C	FR107-FR123	65.4	67.8
Longitudinal bulkhead, port side	6C	FR123-FR139	53.7	64.8
Longitudinal bulkhead, port side	5C	FR139-FR155	66.2	78.7
Longitudinal bulkhead, port side	4C	FR155-FR171	52.6	59.8
Longitudinal bulkhead, port side	3C	FR171-FR187	77.0	83.6

5. Conclusion

A procedure for assessing both the global and the local strength of the ship structure partially grounded in mud has been presented. It has been illustrated by a practical problem of strength assessment of an aged single hull tanker. The mud buoyancy is imposed as a hydrostatic pressure on the ship bottom. The analysis has been performed by 1D FEM and 3D FEM models. The global strength assessment performed by the 1D FEM model indicates that in this particular case there is practically no bending of the ship hull girder, meaning that the global stresses can be neglected. This is because the ship is supported by the mud and it remains the same in different loading conditions. The von Mises stresses and shear stresses are taken as the representative stresses for the evaluation of structural integrity in the 3D FEM analysis. Locations with the highest stress levels are identified for selected load cases. Despite the selection of the most unfavourable loading conditions, represented by different successive combinations of empty and full cargo tanks, the calculated stresses are below permissible values for all structural members. As expected, the maximum stress levels are regularly obtained in transverse bulkheads of the cargo (central) tanks.

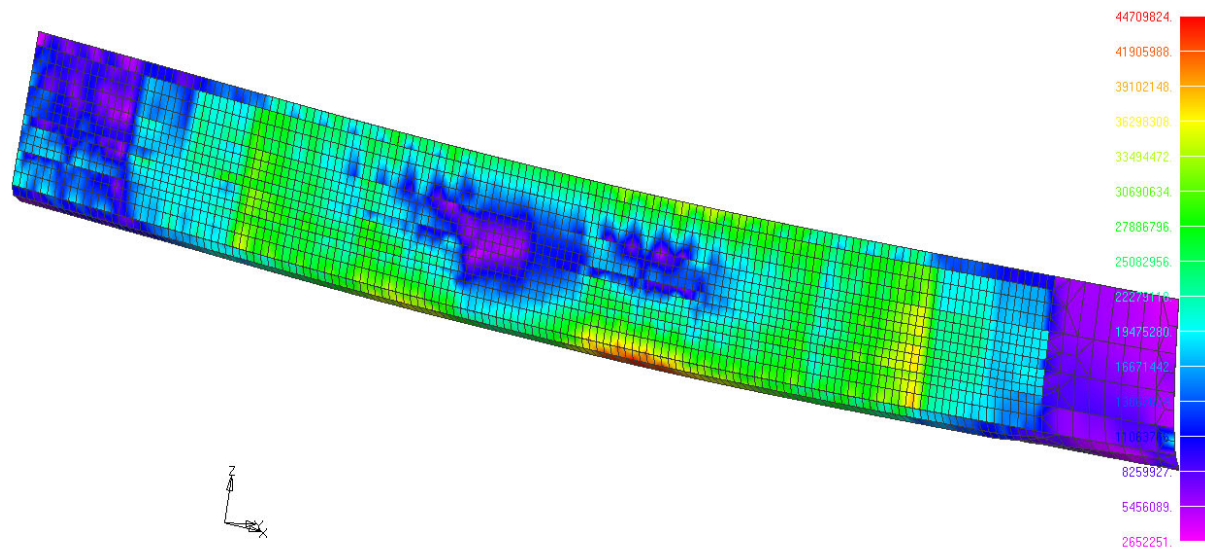


Fig. 18 Von Mises stresses in the starboard outer shell of the ship, LC4

The additional value of the paper is in the physically consistent theoretical model that can be used for determining the reaction pressures of sunken ships in salvaging operations, as well as for similar problems of sunken vessels.

Acknowledgement

The investigation presented in this paper is funded by the Adriatic Tank Terminals d.o.o. Publication of this paper is also supported by the National Research Foundation of Korea (NRF) grant funded by the Korea government (MSIP) through GCRC-SOP (No. 2011-0030013), and within the project Green Modular Passenger Vessel for Mediterranean (GRiMM), funded by the Croatian Science Foundation (Project No. 2017-05-UIP-1253).

REFERENCES

- [1] Yin J and Fan L. Survival analysis of the world ship demolition market. *Transport Policy* 2018; 63: 141-156. <https://doi.org/10.1016/j.tranpol.2017.12.019>
- [2] Stott P. A retrospective review of the average period of ship ownership with implications for the potential payback period for retrofitted equipment. *Proc IMechE Part M: J Eng Maritime Environment* 2013; 228(3): 249-261. <https://doi.org/10.1177/1475090213486096>
- [3] Schøyen H, Burki U, Kurian S. Ship-owners' stance to environmental and safety conditions in ship recycling. A case study among Norwegian shipping managers. *Case Studies on Transport Policy* 2017; 5(3): 499-508. <https://doi.org/10.1016/j.cstp.2017.06.003>
- [4] Alcaide JI, Rodriguez-Diaz E, Piniella F. European policies on ship recycling: A stakeholder survey. *Marine Policy* 2017; 81: 262-272. <https://doi.org/10.1016/j.marpol.2017.03.037>
- [5] Choi JK, Kelley D, Murphy S, Thangamani D. Economic and environmental perspectives of end-of-life ship management. *Resources, Conservation and Recycling* 2016; 107: 82-91. <https://doi.org/10.1016/j.resconrec.2015.12.007>
- [6] Kawamura Y, Sumi Y. Information system for structural integrity of ships. *Proc IMechE Part M: J Eng Maritime Environment* 2005; 219(2): 93-106.
- [7] Eliopoulou E, Papanikolaou A, Diamantis P, Hamann R. Analysis of tanker casualties after the Oil Pollution Act (USA, 1990). *Proc IMechE Part M: J Eng Maritime Environment* 2012; 226(4): 301-312. <https://doi.org/10.1177/1475090212437293>
- [8] Wirsching PH, Ferencic J, Thayamballi A. Reliability with respect to ultimate strength of a corroding ship hull. *Marine Structures* 1997; 10(7): 501-518. [https://doi.org/10.1016/s0951-8339\(97\)00009-9](https://doi.org/10.1016/s0951-8339(97)00009-9)

- [9] Saad-Eldeen S, Garbatov Y, Guedes Soares C. Strength assessment of a severely corroded box girder subjected to bending moment. *J Constr Steel Res* 2014; 92: 90-102. <https://doi.org/10.1016/j.jcsr.2013.09.010>
- [10] Ventikos NP, Sotiralis P, Drakakis M. A dynamic model for the hull inspection of ships: The analysis and results. *Ocean Eng* 2018; 151: 355-365. <https://doi.org/10.1016/j.oceaneng.2017.11.020>
- [11] Ivošević Š, Meštrović R, Kovač, N. Probabilistic estimates of corrosion rate of fuel tank structures of aging bulk carriers. *Int J Nav Archit Ocean Eng* 2018. <https://doi.org/10.1016/j.ijnaoe.2018.03.003>
- [12] Paik JK, Thayamballi AK. Ultimate strength of ageing ships. *Proc IMechE Part M: J Eng Maritime Environment* 2002; 216(1): 57-77. <https://doi.org/10.1243/147509002320382149>
- [13] Rahbar-Ranji A. Ultimate strength of corroded steel plates with irregular surfaces under in-plane compression. *Ocean Eng* 2012; 54: 261-269. <https://doi.org/10.1016/j.oceaneng.2012.07.030>
- [14] Vladimir N, Senjanović I, Alujević N, Tomašević S, Cho DS. Strength assessment of an aged single hull tanker grounded in mud and used as port oil storage, Proceedings of the 4th International Conference on Maritime Technology and Engineering MARTECH 2018 – Progress in Maritime Engineering and Technology, Lisbon, Portugal, 2018; 345-356. <https://doi.org/10.1201/9780429505294-40>
- [15] Mansour Youssef SA and Paik JK. Hazard identification and scenario selection of ship grounding accidents. *Ocean Eng* 2018; 153: 242-255. <https://doi.org/10.1016/j.oceaneng.2018.01.110>
- [16] Gray W. Raising titans: How do you salvage a mega-ship?. *New Scientist* 2013; 220(2944): 48-51. [https://doi.org/10.1016/s0262-4079\(13\)62748-7](https://doi.org/10.1016/s0262-4079(13)62748-7)
- [17] Lee CS, Yoon HS, Kim D, Na WB. Lifting forces required to salvage a sunken vessel and caisson and their response to bottom friction, buoyancy release, surface tension, water capture and water release. *Ocean Eng* 2016; 125: 82-89. <https://doi.org/10.1016/j.oceaneng.2016.08.008>
- [18] Senjanović I and Vladimir N. Physical insight into Timoshenko beam theory and its modification with extension. *Struct Eng Mech* 2013; 48(4): 519-545. <https://doi.org/10.12989/sem.2013.48.4.519>
- [19] Senjanović I, Tomašević S, Vladimir N. An advanced theory of thin-walled girders with application to ship vibrations. *Mar Struct* 2009; 22: 387-437. <https://doi.org/10.1016/j.marstruc.2009.03.004>
- [20] Senjanović I. *Finite element method in analysis of ship structures*, University of Zagreb, Zagreb, 2002. (textbook, in Croatian).
- [21] Cheung YK. *Strip Method in Structural Analysis*, Pergamon Press, 1976.
- [22] Fan Y and Senjanović I. *STIFF, User's Manual*, University of Zagreb, Faculty of Mechanical Engineering and Naval Architecture, Zagreb, Croatia, 1990.
- [23] MSC. 2005. *MSC.NASTRAN2005: Installation and Operations Guide*, MSC Software.
- [24] CRS. 2016. *Rules for Classification of Ships, Part 2 – Hull*, Croatian Register of Shipping, Split, Croatia.

Submitted: 31.7.2018

Accepted: 10.12.2018

Nikola Vladimir
Ivo Senjanović
Neven Alujević
Faculty of Mechanical Engineering and
Naval Architecture, Ivana Lucica 5, 10000
Zagreb, Croatia, nikola.vladimir@fsb.hr
Dae-Seung Cho
Pusan National University, 63 beon-gil 2,
Busandaehak-ro, Geumjeong-gu, Busan,
609-735, Korea
Jose Luis Mantari Laureano
Faculty of Mechanical Engineering,
Universidad Nacional de Ingeniería (UNI),
Avenida Tupac Amaru 210, Rimac, Lima,
Peru, jmantari@uni.edu.pe